Journal of Scientific & Industrial Research
Vol. 82, July 2023, pp. 776-782
DOI: 10.56042/jsir.v82i07.1863

Modeling and Optimization of a Peano-HASEL Actuator Peristaltic Pump

Onat Halis Totuk[1,2]* & Selçuk Mıstıkoğlu[2]
[1]Mechanical Engineering Department, Cankaya University, Ankara, Turkey
[2]Mechanical Engineering Department, Iskenderun Technical University, Hatay, Turkey

Received 12 August 2022; revised 23 May 2023; accepted 09 June 2023

Peano-Hasel (hydraulically amplified self-healing electrostatic) pumps are crucial devices with unique mechanisms and versatile applications. They simulate muscle contractions to move fluids or materials through tubes. The Peano-Hasel method, a specific design, achieves flow by compressing a segmented tube externally. Exploring the design aspects of Peano-Hasel pumps can lead to advancements in optimizing their performance, efficiency, reliability, and control systems. This paper presents a novel method of peristaltic pumping on soft pipes using Peano-HASEL actuators. In the study, a design evaluation of an external ring-type pump over a PDMS (Polydimethylsiloxane - commonly referred to as silicone) tube containing Newtonian fluids is made, and a novel multi-pouch ring shape design is proposed. Our method utilizes a peripheral and compact design that allows for more efficient sinusoidal pumping action. The close proximity of the rings in the longitudinal direction enhances the effectiveness of the pumping process. The actuator is analytically modeled and optimized for maximum areal contraction and flow rate using a differential evolution algorithm. A MATLAB Simulink Simscape model is generated, and the system is simulated. As a result, an optimal solution for the number of pouches was found to be eight, considering ring geometry and applicability. It was also seen from the simulation that a sinusoidal squeezing scheme of a ring-type pump creates the desired action. Based on the analytical model presented, it has been demonstrated that the optimal flow rate is achieved when there are eight pouches, and they are fully circular after being energized.

Keywords: Analytical modelling, Evolution algorithm, Newtonian fluid, PDMS tube, Simulink simulation

Introduction

The entire robotics scene diverted from hard to soft, meaning rigid kinematics, to biomimetically inspired soft material sensed and controlled movements. Recurring and recent advances in the material and manufacturing technologies of soft and smart materials also accelerated the subject. Like Rigid robotics, soft robotics rely upon sensors and actuators. The development of every new sensor, actuator, and hybrid advance brings new usage areas and starts a chain reaction like dominoes. One can discard many disadvantages of softness, such as control, mutability, and compatibility, compared to the advantages, such as lightweight, cobot, and flexibility features. Moreover, these disadvantages seem to disappear as the research on the subject expands. The main categories of robots are hard and hyper-redundant. Soft robotics is a second-level subcategory of the hyper-redundant class. Unlike robots with rigid kinematic chains, soft robots have elasticity. The elasticity can be low or high depending on the concept, but the key factor is high deformability.

In the last decades' robotics has come to a level where the technology is excellent and robust in the name of accuracy and control. However, this knowledge depends on the theory that robots are made out of rigid bodies' kinematic chains. With recent advances in the manufacturing methods of soft and smart materials and nonlinear modeling, soft robotics has been rising as an emerging research topic. Global article indices show that soft robotics is becoming more popular among researchers.[1]

The use of soft materials in biomimetics is now essential. Biomimetics is the art and science of using the behavior of nature to advance engineering solutions. Soft robots imitate biological systems that are soft-bodied naturally.[2–6]

Actuators or transducers are essential parts of robotics in the sense that no intended aim can be reached without them. Actuation is an outcome of direct physical action upon the process, such as exerting a force or application of limitation. Various actuating devices such as solenoids, ac, dc, or stepper motors, pneumatic devices, piezoelectric motors, and

*Author for Correspondence
E-mail: onattotuk@cankaya.edu.tr

electrohydraulic devices are used in regular robotics. These take a relatively weak command signal and convert a kind of energy to another such as electrical to mechanical. Soft robotics studies added many different methods of actuation to the conventional ones listed above. Electrical actuation, electrothermal, shape memory alloy, pneumatic, hydrogel, and polymer-based actuation systems are introduced. In most of, the flexibility of polymers plays a vital role as a foundation.

Electrostatic actuators deserve special attention among the main lines of electrical actuation. Electrohydraulic HASEL (hydraulically amplified self-healing electrostatic) actuators are a new type employing electrostatic forces to move a dielectric liquid contained in a soft jacket to create shape change. Saif *et al*. developed an analytical model for forecasting the electrostatically actuated micropump state at equilibrium.[7] The model contains the minimization of the total energy, which can comprise capacitive energy, the diaphragm's strain energy, and the energy of the fluid. This study might be considered a start-up for HASEL. Kellaris *et al*. wrote about a soft electrohydraulic transducer named hydraulically amplified self-healing electrostatic (Peano-HASEL) actuators.[8] Besides, they mentioned structure, working principles, and usage possibilities. Acome *et al*. show the advantages of using HASELs with a muscle-like performance produced by standard techniques and easily obtainable materials.[9] They also provided some prototype design ideas and established the durableness of the system. Mitchell *et al*. wrote a toolkit for prototyping, producing, testing, and using HASELs with muscle-like performance on three basic working modes of actuation: expansion, contraction, and rotation.[10] Rothemund *et al*. researched the impact of inhomogeneous zipping on the performance of Peano-HASEL actuators. Kellaris *et al*. developed an analytical model for understanding the effect of geometry and material type on the performance of HASEL actuators by minimizing the total energy method.[11] Manion *et al*. present donut-type HASEL actuators that are entirely produced using 3D printers.[12] They also provide a coupled electrical, hydraulic, and nonlinear elastic model tested and validated for estimating the actuation strain. Ly *et al*. provide a novel circuit design that reduces the cost by removing the requirement for high-voltage sensing components with accurate results on circular DEAs (dielectric elastomer actuators) and HASELs.[13] Rothemund *et al*. analyzed the dynamics of HASELs using experiments and scaling analysis.[14] They prepared a timescale that contains the effects of geometry, material, and actuation speed with a model of dynamic behaviors. Rothemund *et al*. summarized recent progress and future opportunities of HASEL Artificial Muscles for a New Generation of Lifelike Robots.[15] Lin & Liu applied dielectric elastomers to a spiral probosci's actuator to achieve a coiling effect.[16] Wang *et al*. made a summary of recent progress in artificial muscle for interactive soft robotics.[17] Wissman *et al*. studied optical lens fabrication using HASEL actuators.[18] Hau *et al*. created a high-force application concept for a dielectric elastomer membrane actuator.[19]

While Saif *et al*. made an electrically actuated micropump, they have not used the HASEL approach and employed a diaphragm over a cavity.[7] The applications of HASEL in Kellaris *et al*. and Rothemund *et al*. are only on linear pull type, Acome *et al*., Mitchell *et al*. studied curling and bending type of HASEL actuators.[8–10,14,20] Cacucciolo *et al*. invented a stretchable pump based on charge-injection electrohydrodynamics, and the invention is on fluid-driven soft systems.[21] The system is based on the dielectric fluid in the channel and is accelerated by means of a high DC electric field.

The purpose of this paper is to evaluate a design of a non-intervened external fluidic pump that can be implemented using Peano-HASEL fundamentals. Combining sensing capabilities of soft robotics and the flexible and selective actuation methods of Peano-HASEL would lead to a novel way of pumping fluids externally in small-sized soft pipes. The bridge and interaction between sensing and movement creation can be orchestrated by smart decision-making components such as microcontrollers. This will enable the response robotic pump to be flexible in accuracy and control while employing smart and self-reacting materials. This paper first gives a brief overview of the art of soft robotics and actuators. Then a novel multi-pouch ring shape design for peristaltic pumping is suggested. The actuator is analytically modeled and optimized for maximum areal contraction, which will, in turn, create maximum flow rate. Afterward, a MATLAB Simulink Simscape model is made, and the system is simulated. Finally, results of optimization and simulation are tabulated. The optimization study is intended to the bullseye target area of the further studies on experimentation and focuses the effort on eliminating the diversion.

Method

A Newtonian fluid containing PDMS (Polydimethylsiloxane - commonly referred to as silicone) pipe is planned to peristaltically pumped. Compressing the pipe will decrease the cross-sectional area and will force the incompressible fluid to a motion. The direction of flow is determined by consecutive compressions created by external squeezing force resulting in a peristaltic actuation. Here we use three-stage actuated rings as shown in Fig. 1(a). These actuators to be actuated sinusoidally, as shown in Fig. 1(b).

Each ring actuator is designed of multiple Peano-Hasel cells. These types of cells are filled with incompressible and dielectric fluid in a free pouch form. Some portion of the pouch is covered with electrodes. When these electrodes are charged with opposite high voltages, they attract electrostatically, causing zipping. In this way, dielectric fluid is moved to the electrodeless portion of the pouch, creating a

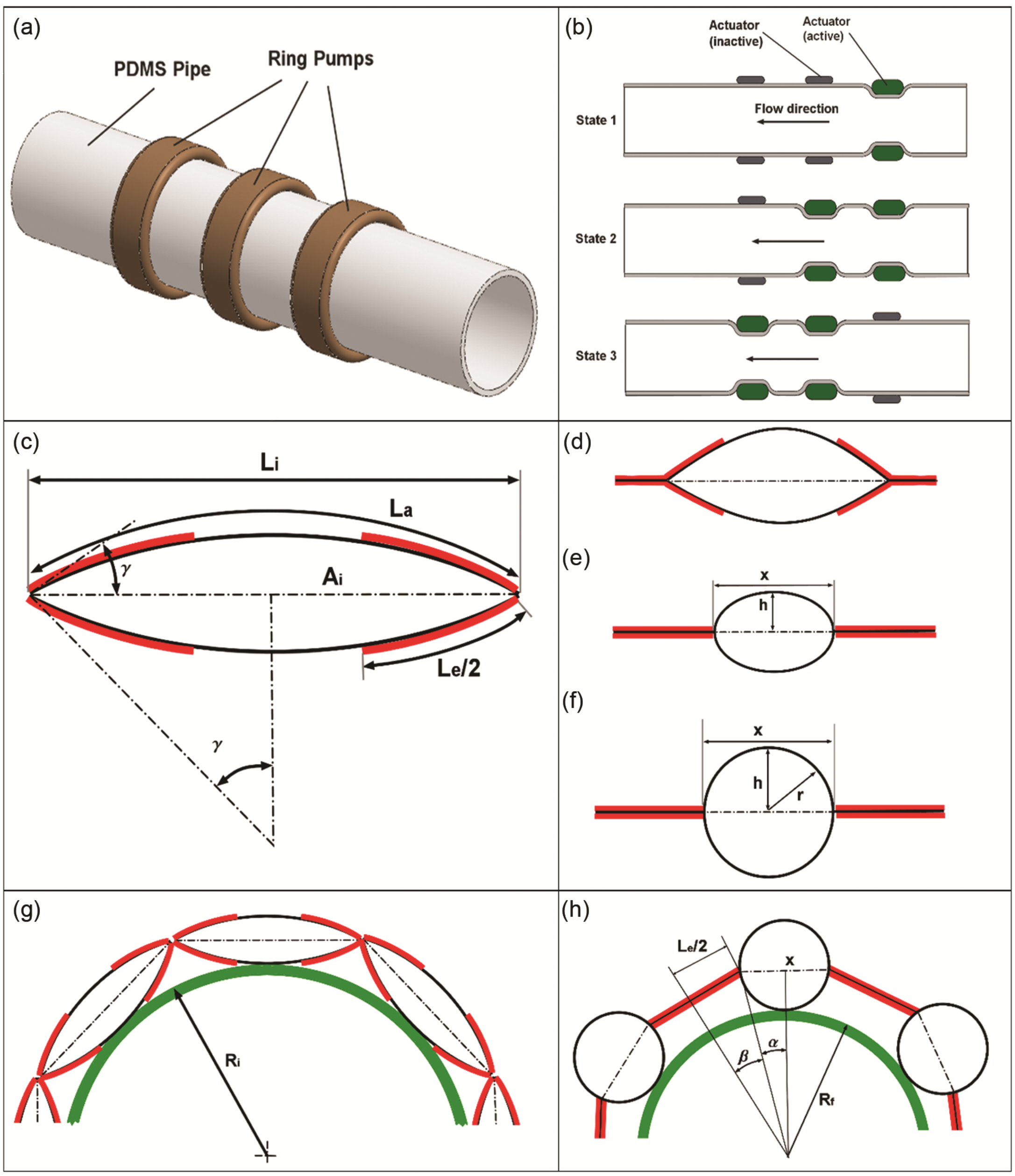

Fig. 1 — Design and analytical model of ring actuated peristaltic pump; a) Ring Placement, b) Actuation Sequence, c) Parametrization of the pouch shape in the inactive state, d) Partially actuated state, e) Fully actuated bulged state, f) Fully actuated circular state, g) Peripheral cell configuration in the inactive state, h) Fully actuated state

bulging shape change. Using this effect on the periphery of an elastic pump would, in turn, create desired squeezing force and action.

Due to the nature of the problem at hand, static and dynamic force calculations are omitted because the main interest is how much fluid will be transferred from one part of the pouch to the other after the zipping action. A cross-section of a cell at the initial position is shown in Fig. 1(c), where the angle of the Peano pouch bulge is γ, which is also the half of the chord covering angle, chord length is L_i, arc length is L_a, area of the pouch section is A_i, and electrode length is L_e. Partially actuated, fully actuated non-circular (bulged) output, and fully actuated circular output of the cell pouches are shown in Fig. 1(d), Fig. 1(e), and Fig. 1(f) respectively when they are electrostatically loaded with high voltage. Here h is the height of the bulge, x is the width (chord length) of the bulge, and r is the circular output radius.

Multiple cells are to be placed around the pipe periphery to create compressive action when the cells are actuated, as shown in Fig. 1(g). Fully actuated cells with compressive action on the pipe is shown in Fig. 1(h) where R_i is the initial radius of the pipe. R_f is the pipe's final radius, α is the bulge angle, and β is the electrode angle.

Three parameters are needed to find the change of the cross-sectional inner area of the tube subjected to force from the HASEL actuators. These are γ_0: initial angle of the pouch, n: number of actuators around the pipe, η: the ratio of electrical coverage ($\boldsymbol{L_e}$) to the total length of the HASEL L_a. The initial length of the HASEL actuator can be found using Eq. (1)

$$L_i = \frac{2R}{\mathrm{Cot}[\frac{\pi}{n}]+\mathrm{Cot}[\gamma_0]-\mathrm{Csc}[\gamma_0]} \quad \ldots (1)$$

where, R is the initial radius of the inner tube

Then the arc length L_a can be calculated using Eq. (2)

$$L_a = \frac{L_i\gamma_0}{\mathrm{Sin}[\gamma_0]} \quad \ldots (2)$$

The initial height of the cell can be calculated using Eq. (3)

$$h_i = \frac{L_a}{2\gamma_0} \times (1 - \mathrm{Cos}[\gamma_0]) \quad \ldots (3)$$

then the initial area can be found as in Eq. (4)

$$\mathrm{Ai} = \frac{1}{2} \times (\frac{L_a}{2\gamma_0})^2 (2\gamma_0 - \mathrm{Sin}[2\gamma_0]) \quad \ldots (4)$$

Then the value of γ after the electrical force is applied can be found by solving Eq. (5)

$$\mathrm{Ai} == \frac{1}{2} \times (\frac{L_a(1-\eta)}{2\gamma_f})^2 (2\gamma - \mathrm{Sin}[2\gamma]) \quad \ldots (5)$$

where, η is the ratio of L_e/L_a, γ_f is the final value for the pouch angle.

The final value of the γ, the change in the lateral length (x), and the final vertical height (hf) of the pouch can be calculated utilizing Eq. (6) and Eq. (7), respectively

$$x = \frac{L_a(1-\eta)}{\gamma} \times \mathrm{Sin}[\gamma] \quad \ldots (6)$$

$$h_f = \frac{L_a(1-\eta)}{2\gamma} \times (1 - \mathrm{Cos}[\gamma]) \quad \ldots (7)$$

the total length of the pouch can be calculated using Eq. (8)

$$L_f = L_a(\eta) + x \quad \ldots (8)$$

Then the angle of pouches in the final position (α) that is shown in Fig. (1c) can be calculated using Eq. (9)

$$\alpha = \mathrm{ArcCot}[\frac{(L_a\eta + x\,\mathrm{Cos}[\frac{\pi}{n}])\mathrm{Csc}[\frac{\pi}{n}]}{x}] \quad \ldots (9)$$

the final outer radius of the tube can be found from Eq. (10)

$$R_f = \frac{0.5x}{\mathrm{Tan}[\alpha]} - \mathrm{hf} \quad \ldots (10)$$

Then the initial area and the final cross-sectional area of the tube can be found using Eq. (11) and Eq. (12), respectively

$$\mathrm{ICA} = \pi \times R^2 \quad \ldots (11)$$

$$\mathrm{FCA} = \pi {R_f}^2 \quad \ldots (12)$$

Using ICA and FCA percentage change of the cross-sectional area can be found, which is also the objective function of the optimization problem.

$$\text{percent change} = \frac{\mathrm{ICA}-\mathrm{FCA}}{\mathrm{ICA}} \times 100 \quad \ldots (13)$$

Optimization is applied to create maximum cross-sectional area reduction. This would, in turn, produce maximum flow in the pipe. The number of cells n, initial state value γ_0, and the ratio of L_e to L_a η are used as variables to get the desired result. Since the equation is nonlinear, non-continuous, and noisy in nature, a differential evaluation algorithm is employed. In the further study, having an increased number of parameters and multi-dimensional considerations, other metaheuristic algorithms such as bee, dolphin, firefly, or genetic might be employed where necessary.

The objective function of the optimization will be $f(\gamma_0, \eta)$ = percent change of crossectional area

Subject to constraints

$$\eta \leq 1 - \sqrt{\frac{\pi}{2} * \left(\frac{\gamma_0 - \mathrm{Sin}[\gamma_0]\mathrm{Cos}[\gamma_0]}{\gamma_0{}^2}\right)}, \eta > 2\gamma_0/\pi$$

After achieving the optimization, the parameters will be used for a design that will be simulated in MATLAB Simulink Simscape.[22]

Results and Discussion

The results of optimization method are shown in Table 1 in terms of the number of cells n, initial state value γ_0, and the ratio of L_e to L_a η. For the number of cells between 7 to 14, an even number of cells gives a higher area change than the odd number of cells. The general trend shows that as the number of cells increases, the area changes decreases. With these results in mind n = 8 is selected for the simulation and Fig. 2 shows the created contour plot of area change percentage accordingly.

Table 1 — Optimization parameters and max area change

n	$\Upsilon_0/(\pi/2)$	η	Area Change (%)
7	0.23	0.38	49.85
8	0.28	0.32	52.20
9	0.23	0.38	47.54
10	0.29	0.31	50.30
12	0.29	0.32	48.55
14	0.26	0.35	46.14

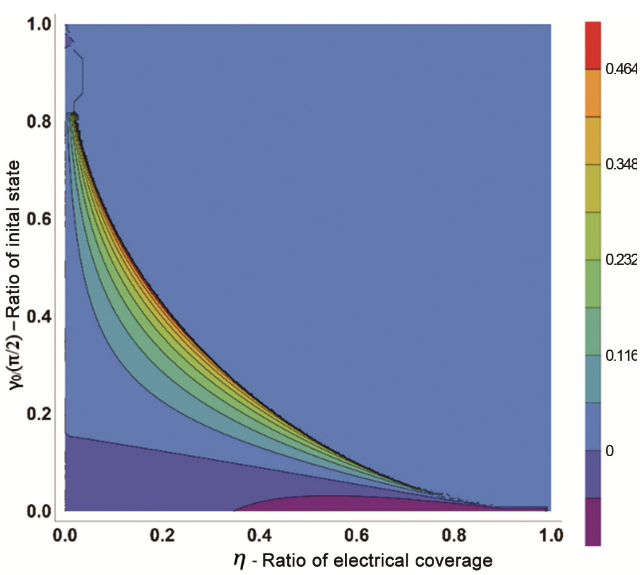

Fig. 2 — Contour plot of area change percentage when n = 8

To simulate peristaltic pumping action, the multi-physics simulation tool, Simscape, is used. The motion is mechanically generated and controlled by a series of pistons. The mechanically created peristaltic wave in the pipe, in turn, generates the flow in a sinusoidal manner. The system model schematics are shown in Fig. 3(a). This system consists of components including the individual pumping cells and loads connected in series, whose behavior is given by component-level representations depicted in Fig. 3(b). Finally, the simulated model of the Peano-HASEL Motion is shown in Fig. 3(c), where equivalent piston diameter is 78.5×10^{-6} m^2, piston length is 0.005 m, and check valve cracking pressure is 0.3×10^{-5} Pa. Simulation results as per volume increase and mass flow rate in time are given Fig. 4(a) and Fig. 4(b), respectively. The flow rate in the tube is found as 2.5×10^{-5} m^3.

We have presented a design and simulation study of a Peano-HASEL actuated peristaltic pump consisting of three compressive rings. The compressive rings are planned to be made of electrostatically activated varying numbers of cells. The number of cells is optimized with maximizing area reduction in the pipe. The reduction of area effectively goes around 50%, enabling pumping action to be started under the no backflow assumption. No backflow assumption is based on consecutive squeezes performed to create sinusoidal action. Two consecutive squeezes will cause enough drop in diameter so that liquid will move away from these in a peristaltic direction. Three Peano-HASEL rings with consecutive compressive action with the proposed sequence create a positive peristaltic pumping result, as seen in the simulation model. The increasing number of rings would be assumed to smoothen the curve of the sinus output of the pumping.

The closest application to our novel design form is created by Wang *et al.*[17] as Artificial Circular Muscle (ACM). The form of HASEL actuator, in this case, made longitudinal in the direction of flow, being lengthy and harder to apply. Our novel method is peripheral and smaller in the longitudinal direction so that sinusoidal pumping action can be achieved more effectively, rings being closer to each other. Effective volume change in this method is shown to be 17.7%, owing to the partial compression of the actuator assuming 59% area reduction. On the other hand, our novel method with nearly 50% area reduction is not

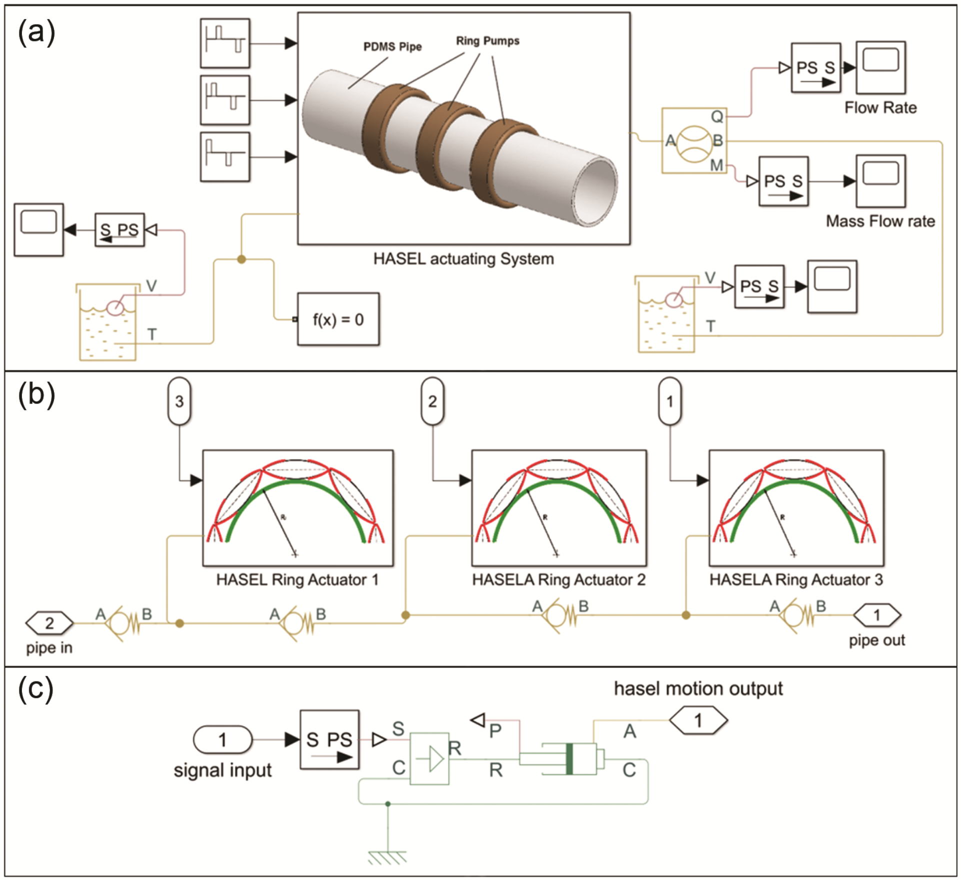

Fig. 3 — Simulation model: (a) System schematics, (b) Pumps in a series configuration, (c) Pump model

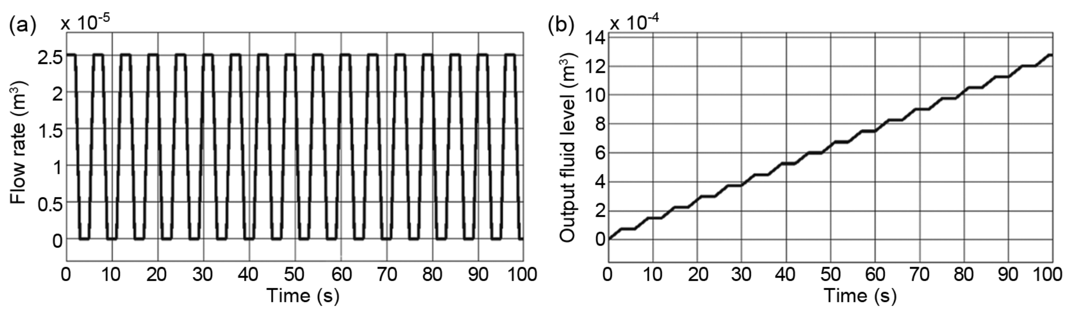

Fig. 4 — Simulation results: (a) Volume increase, (b) Mass flow rate

affected by a length change, thus creating a 50% volumetric change per unit length.

Conclusions

In this study a multi-pouch ring shape design has been developed for peristaltic pumping, utilizing a peripheral and compact design to achieve more efficient sinusoidal pumping action. Through analytical modeling and optimization using a differential evolution algorithm, the actuator is optimized for maximum areal contraction and flow rate. A MATLAB Simulink Simscape model is generated, and the system is simulated to validate the proposed design. The results demonstrate that an optimal solution for the number of pouches in the pump is eight, considering ring geometry and applicability. The simulation confirms that a sinusoidal squeezing scheme of a ring-type pump generates the desired pumping action.

It was apparent that the Peano-HASEL actuator has been an excellent biomimetic approach to a muscle-like actuation needed in a soft pipe containing environments like the human body. Exploring the use of muscle-like actuators for external pumping action in bodily fluids, such as blood, can be a promising alternative. Further studies could investigate the transition from Newtonian to non-Newtonian flow characteristics in order to enhance the effectiveness of these actuators. These improvements would enable the next-generation soft container pumping requirements.

References

1 Bao G, Fang H, Chen L, Wan Y, Xu F, *Yang Q & Zhang L*, Soft robotics: Academic insights and perspectives through bibliometric analysis, *Soft Robot*, **5(3)** (2018) 229–241.

2 Kim S, Laschi C & Trimmer B, Soft robotics: A bioinspired evolution in robotics, *Trends Biotechnol*, **31(5)** (2013) 287–294.

3 Coyle S, Majidi C, LeDuc P & Hsia K J, Bio-inspired soft robotics: Material selection, actuation, and design, *Extrem Mech Lett*, **22** (2018) 51–59.

4 Corucci F, Cheney N, Kriegman S, Bongard J & Laschi C, Evolutionary developmental soft robotics as a framework to study intelligence and adaptive behavior in animals and plants, *Front Robot AI*, **4(7)** (2017) 1–7.

5 Gravish N & Lauder G V, Robotics-inspired biology, *J Exp Biol*, **221(7)** (2018) 1–8.

6 Paley D A, Majidi C, Tytell E & Wereley N, Bioinspired soft robotics: Preface to the special issue, *Bioinspir Biomim*, **11(2)** (2016) 020401.

7 Saif M T A, Alaca B E & Sehitoglu H, Analytical modeling of electrostatic membrane actuator for micro pumps, *J Microelectromechanical Syst*, **8(3)** (1999) 335–345.

8 Kellaris N, Venkata V G, Smith G M, Mitchell S K, & Keplinger C, Peano-HASEL actuators: Muscle-mimetic, electrohydraulic transducers that linearly contract on activation, *Sci Robot*, **3(14)** (2018) 1–11.

9 Acome E, Mitchell S K, Morrissey T G, Emmett M B, Benjamin C, King M, Radakovitz M & Keplinger C, Hydraulically amplified self-healing electrostatic actuators with muscle-like performance, *Science*, **359(6371)** (2018) 61–65.

10 Mitchell S K, Wang X, Acome E, Martin T, Ly K, Kellaris N, Venkata V G & Keplinger C, An easy-to-implement toolkit to create versatile and high-performance HASEL Actuators for untethered soft robots, *Adv Sci*, **6(14)** (2019) 1900178.

11 Rothemund P, Kellaris N & Keplinger C, How inhomogeneous zipping increases the force output of Peano-HASEL actuators, *Extrem Mech Lett*, **31** (2019) 100542.

12 Manion C A, Patel D K, Fuge M & Bergbrieter S, *Modeling and Evaluation of Additive Manufactured HASEL Actuators*, IROS 2018 Conference (Madrid, Spain)

13 Ly K, Kellaris N, McMorris D, Johnson B K, Acome E, Sundaram V, Naris M, Humbert J S, Rentschler M E, Keplinger C & Correll N, Miniaturized circuitry for capacitive self-sensing and closed-loop control of soft electrostatic transducers, *Soft Robot*, **58(12)** (2020) soro.2020.0048.

14 Rothemund P, Kirkman S & Keplinger C, Dynamics of electrohydraulic soft actuators, *Proc Natl Acad Sci U S A*, **117(28)** (2020) 16207–16213.

15 Rothemund P, Kellaris N, Mitchell S K, Acome E & Keplinger C, HASEL Artificial muscles for a new generation of lifelike robots—Recent progress and future opportunities, *Adv Mater*, **2003375** (2020) 1–28.

16 Lin PW & Liu CH, Bio-inspired soft proboscis actuator driven by dielectric elastomer fluid transducers, *Polymers (Basel)*, **11(1)** (2019) 142.

17 Wang X, Mitchell S K, Rumley E H, Rothemund P & Keplinger C, High-strain peano-HASEL actuators, *Adv Funct Mater*, **30(7)** (2020) 1–9.

18 Wissman J P, Ikei A K & Rohde C A, *Hydraulically Amplified Self-Healing Electrostatic (HASEL) Inspired Actuators* (2021), https://doi.org/10.48550/arXiv.2102.13039.

19 Hau S, Rizzello G & Seelecke S, A novel dielectric elastomer membrane actuator concept for high-force applications, *Extrem Mech Lett*, **23** (2018) 24–28.

20 Kellaris N, Venkata V G, Rothemund P & Keplinger C, An analytical model for the design of Peano-HASEL actuators with drastically improved performance, *Extrem Mech Lett*, **29** (2019) 100449.

21 Cacucciolo V, Shintake J, Kuwajima Y, Maeda S, Floreano D & Shea H, Stretchable pumps for soft machines, *Nature*, **572 (7770)** (2019) 516–519.

22 Meng Y, Fang Y & Liu C, Research on the virtual prototyping technology of the electric- hydraulicmechanical system based on simcape, *ICACTE 2010 - 2010 3rd Int Conf Adv Comput Theory Eng Proc*, **1** (2010) 465–469.